Novel Constant Frequency PWM DC/DC Converter with Zero Voltage Switching for Both Primary Switches and Secondary Rectifying Diodes

In-Dong Kim, Eui-Cheol Nho, and Gyu-Hyeong Cho, *Member, IEEE*

***Abstract*—A new zero voltage switching (ZVS) dc / dc converter operating on constant frequency and having wide linearity is proposed. ZVS operations are achieved not only for the primary switches but also for the secondary rectifier diodes to reduce the switching stresses and losses. The proposed converter also overcomes the other shortcomings of the conventional resonant dc / dc converters such as high VA ratings of devices and passive components, load-dependent dc characteristics, and so on.**

I. Introduction

A number of dc/dc converters employing either zero voltage or zero current high-frequency switching operation have been studied extensively. Resonant-type converters and quasi-resonant-type converters [1]–[3] can operate at high frequencies with low switching loss and low electromagnetic interference (EMI). Thus these converters have merits such as reduced size and weight of the filters and isolation transformers. However, they also have several well-known problems such as high VA ratings of devices and components, variable switching frequency, load-dependent dc characteristics, and complex control. The other converters that are partially resonant only during switching transients appear in the literature [4]–[6]. These partial resonant converters use reactive elements or capacitive snubbers to shape the switching trajectory of the devices to realize zero voltage switching. The reactive elements are not involved in primary power transfer but as act snubbing function only. Thus, VA ratings of the elements and their dissipations due to effective series resistance (ESR) are very low compared with those of the resonant and quasi-resonant converters. However, these converter should be designed considering large ripple current handling capabilities at the output capacitor and high current stresses in the devices because the resonant inductors that act as energy transfer elements have almost triangular current waveforms. In addition, the dc conversion-ratio characteristics are nonlinear and load dependent, although these converters operate at constant switching frequency by utilizing the phase-shift control technique.

In this paper, a new zero voltage switching PWM dc/dc converter that overcomes the shortcomings of the conventional resonant dc/dc converters as mentioned above is proposed. ZVS operations are achieved not only for the primary switches but also for the secondary rectifier diodes to reduce the switching stresses and losses. Besides, the voltage and current stresses of the devices and components in the proposed converter are reduced and always clamped to the supply voltage V_S and the output current I_O, respectively.

II. Preproposed Converter

The basic configuration of the proposed converter, called the "preproposed" converter in this paper, is a full-bridge one with output filter L_O as shown in Fig. 1(a). Each pole is composed of series connected two switches to which resonant capacitors and diodes are connected in parallel. The main role of resonant inductor L_r and the resonant capacitors is to provide the zero voltage switching condition. The filter inductor L_o is large enough to maintain almost constant output current. The typical waveforms of the preproposed converter are represented as shown in Fig. 1(b). In appearance, the preproposed scheme looks like the partial-resonant type converter in the sense that resonant elements L_r, $C_r(C_1 - C_4)$ resonate partially only for the duration of switching transient to ensure zero voltage switching condition. However, the preproposed converter not only gives the partial-resonant operation but also provides several good features as described below.

First of all, one of the features of the preproposed converter results from the current waveform of the resonant inductor. As Fig. 2(a) shows, the series-resonant type converters have the approximately sinusoidal current waveforms of the resonant inductor and the partial-resonant type converters usually generate the triangular current waveform. Thus the peak values of series resonant converter and partial resonant converter become about

Manuscript received November 16, 1990; revised October 11, 1991.

I. D. Kim is with the Rolling Stock R & D Center of Rolling Stock & Heavy Equipment Div., Daewoo Heavy Industries Ltd., Anyang, Kyunggi, Korea 437-040.

E. C. Nho is with Power Tech Ltd., Seoul, Korea 135-230.

G. H. Cho is with the Electrical Engineering Department, Korea Advanced Institute of Science and Technology, Seoul, Korea 305-701.

IEEE Log Number 9202503.

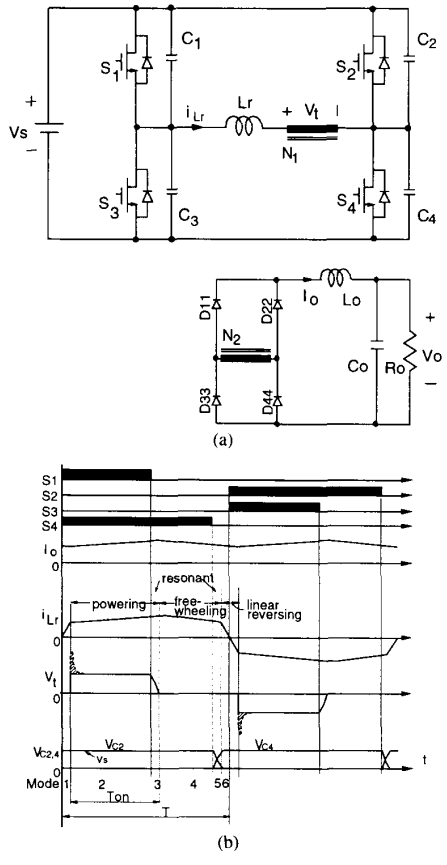

Fig. 1. Preproposed zero-voltage-switching PWM dc/dc converter. (a) Circuit diagram. (b) Typical waveforms (the dotted parts of waveform V_t are the case of considering reverse recovery of off-going output diodes).

$\pi/2$ times and twice as high as the average one, respectively. On the contrary, the preproposed one has the smoothed square current waveform. Its peak value is almost as good as the average one. Therefore, under the same power level the preproposed converter has reduced the peak and rms ratings of all of the devices and reactive elements and requires lower ripple current capability at the output capacitor.

The smoothed square waveform of the preproposed converter is obtained by particular operations of two inductors L_r and L_o through either series-connection mode or decoupled mode. Fig. 2(b) represents the equivalent circuit of the preproposed converter during a time interval (from mode 2 to 3) where both inductors are series connected, and thus resonant inductor current i_{Lr} remains clamped to the output filter inductor current I_O:

$$i_{Lr}(t) = I_O. \tag{1}$$

On the other hand, during a subsequent time interval (from mode 4 to 1), the preproposed converter is divided into two isolated equivalent circuits by decoupling two inductors through a short circuit of a diode bridge as shown in Fig. 2(c). In this interval, the output current I_O

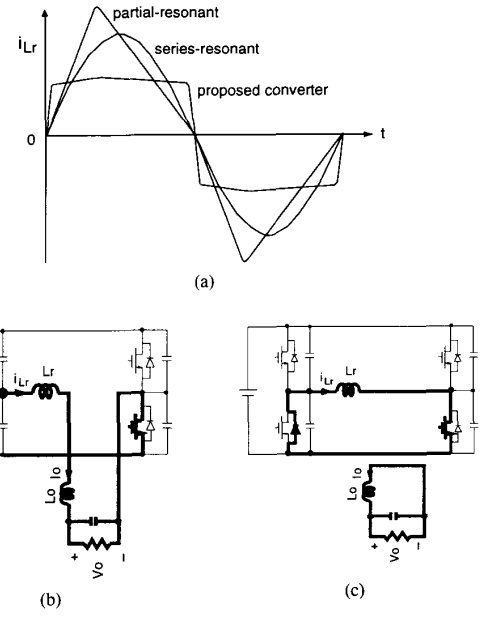

Fig. 2. Characteristics of a preproposed converter. (a) Current waveforms of resonant inductor. (b) Equivalent circuits during series-connection of L_r and L_O (*from mode 2 to mode 3*). (c) During separation (*from mode 4 to mode 1*).

is kept almost constant by freewheeling through shorted diodes and load R_o whereas the resonant current i_{Lr} becomes partially resonant and linearly decreases via zero to the output current I_O, or

$$|i_{Lr}(t)| < I_O. \tag{2}$$

When the resonant current i_{Lr} reaches to the output current I_O, both inductors are series connected again and thus the next cycle begins. Therefore, the current stresses of devices and components are low and always clamped to the output current I_O.

When the two inductors are series connected, power is transferred from source to load, where there is no power transfer when the inductors are decoupled. For that reason, the power transfer mechanism of the proposed converter can be represented by powering and freewheeling operations similar to that of the switched-mode PWM converter. The output power can be regulated by varying the duty ratio of powering and freewheeling intervals. The duty ratio control or pulse width modulation control enables constant switching operation and results in linear and load-independent dc characteristics. Even though this basic converter provides many good features as mentioned above, it severely suffers from reverse recovery problem of the diodes as typically encountered in many power converters.

III. Recovery Problem in the Output Diodes

Many nontrivial limitations of the diodes are caused by the property that is universal for all of the silicon devices. The property is excess stored charge needed to sustain

forward current flowing. The most important diode limitation that arises due to the stored charge is reverse recovery. The diode reverse recovery phenomena in the power converters have been among the most troublesome and acute problems faced by converter designers. The preproposed converter also suffers from the reverse recovery phenomenon during transition transients between modes 1 and 2. Fig. 3 shows the equivalent circuit and corresponding waveforms during reverse recovery. During mode 1 $[t_0, t_1]$, the current through the off-going output diodes D22 and D33 are linearly decreased while the resonant inductor current is increased from zero to I_O. At time instant t_1, the diode reverse recovery process is initiated and thus the diode current I_d builds up reversely at a rate limited by a resonant inductor L_r, or

$$\frac{dI_d}{dt} = \frac{V_S}{L_r} \tag{3}$$

until the stored charges of the output diodes are completely removed. The peak reverse diode current can be found to be

$$I_{RP} = \sqrt{\frac{V_S I_O \tau_S}{L_r}} \tag{4}$$

where τ_S is the storage time constant of the diode. This process stores excess energy to the resonant inductor and imposes peak current stress $(I_O + I_{RP})$ on the main switch. Subsequent diode snap-off between t_2 and t_3 causes substantially large voltage spike across the off-going output diodes, or

$$V_{\text{spike}} = V_S - L_r \frac{dI_d}{dt} \tag{5}$$

and results in very large dissipations in the output diodes given by

$$P_{\text{loss}} = \frac{1}{T_s} \int_{t_2}^{t_3} V_{\text{spike}} I_d \, dt \tag{6}$$

$$= V_S Q_j f_S + \frac{L_S}{2} I_{RP}^2 f_S \tag{7}$$

where f_S is the switching frequency and Q_j is the reverse recovery charge during snap-off. These problems limit the maximum switching frequency of the converter and result in substantial reduction of system efficiency and reliability.

IV. Proposed Converter

Usually the reverse recovery problem of output diodes D_{11}–D_{44} is inevitable in the transformer coupled inductive filter circuits. Such a problem is eliminated by providing zero voltage switching and spike voltage clamping action for the output bridge diodes. Fig. 4(a) shows the proposed converter having an auxiliary circuit. The auxiliary circuit consist of C_{rr} and diode bridge (D_{a1}–D_{a4}) and gives the solution for the reverse recovery problem of the output bridge diodes by connecting the capacitor C_{rr} to the terminals of another winding of the isolation transformer.

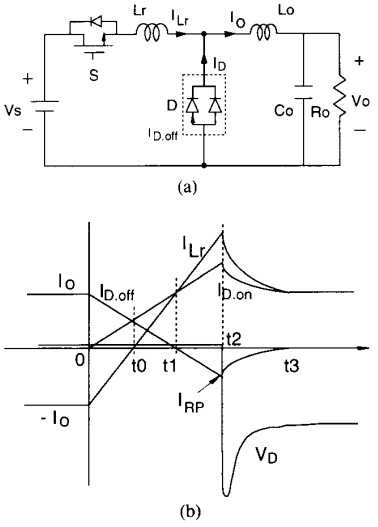

Fig. 3. Illustration of the diode reverse recovery of the preproposed converter. (a) Equivalent circuit during reverse recovery. (b) Characteristic waveforms ($i_{D.on}$: oncoming diode current, $i_{D.off}$: off-going diode current).

The operating waveforms for the auxiliary circuit are shown in Fig. 4(b), including the reverse recovery effect of the off-going output diodes. The resonant inductor current i_{Lr} increases linearly during mode 1 (hereafter, mode numbering is designated related to that of Fig. 5). When the current reaches the output current I_O the reverse recovery current in the off-going output diodes start to conduct reversely. The diode reverse current increases at the rate of change determined by external circuit, or

$$di_{Lr}(t)/dt = V_S/L_r \tag{8}$$

while storing excess energy to the resonant inductor L_r. It ceases increasing when the excess charge of the output diode is extracted. The diode reverse recovery current decays, recovering the reverse voltage-blocking capability. During this decay interval (diode snap-off interval), the diode blocking voltage does not increase suddenly but increases gradually because of the capacitor C_{rr} connected in parallel with the off-going diodes. The blocking voltage of the off-going diodes keeps nearly zero level during the short decay interval providing them zero voltage switching.

In mode 2, the capacitor voltage $V_{C_{rr}}$ (the same as the waveform V_{D33} shown in Fig. 4(b)) increases partially resonant with the excess energy current. When the capacitor voltage v_{Crr} reaches supply voltage V_S, the auxiliary bridge diodes are turned on and thereby clamp the capacitor voltage to supply voltage V_S (mode 3). Finally, the excess energy stored in the resonant inductor returns to the power supply. In this operation, the auxiliary bridge diodes also switch at zero voltage condition. Consequently, the combination of the third isolation winding, L_r, C_{rr}, and the auxiliary diode bridge returns the reverse recovery energy of the output diodes and provides zero

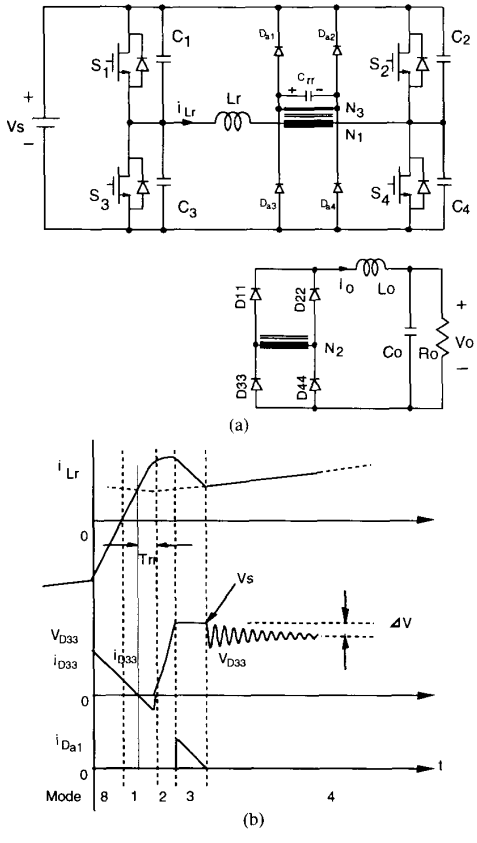

Fig. 4. Proposed zero-voltage-switching PWM dc/dc converter. (a) Circuit diagram. (b) The magnified waveforms of proposed converter including reverse recovery effect of output diodes (T_{rr}: reverse recovery interval). Mode 1 (linear increasing; mode 2 (resonant); mode 3 (clamping); mode 4 (powering); mode 5 (resonant); mode 6 (freewheeling); mode 7 (resonant); mode 8 (linear decreasing).

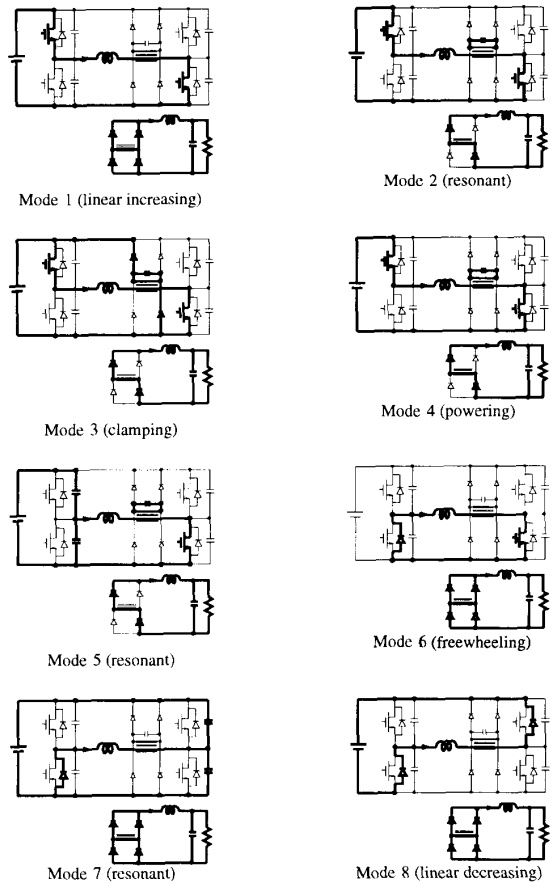

Fig. 5. Topological mode diagrams of proposed converter.

voltage switching and spike voltage clamping to the off-going output diodes. It should be noted, of course, that the proposed converter with auxiliary circuit does not disturb the good features of the preproposed converter at all.

V. Analyses of the Operating Modes

The overall operation of the proposed converter can be divided into powering (mode 4), resonant (modes 2, 5, 7), freewheeling (mode 6), linear increasing, and linear decreasing (modes 1, 8) modes according to the inductor current waveform i_{Lr}. Output capacitor C_O is assumed to be sufficiently large to be replaced by voltage source V_O. The corresponding topological mode diagrams are shown in Fig. 5.

1) *Mode 1 (linear increasing):* This mode occurs with all output bridge diodes conducting, thereby effectively decoupling the resonant circuit and the output circuit. Thus the resonant inductor current increases linearly by the supply voltage and the output current I_O freewheels through the short-circuited output bridge diodes, that is,

$$i_{Lr}(t) = \frac{V_S}{L_r} t \tag{9}$$

$$I_O(t) = I_O(t_0) - \frac{V_O}{L_O} t. \tag{10}$$

2) *Mode 2 (resonant):* When the resonant inductor current i_{Lr} reaches the peak current ($I_O + I_{RP}$), only two output diodes remain conducting state, and the others are turned off under zero voltage switching condition in relation to the resonant operation of L_r and C_{rr}. Zero voltage switching operation eliminates large voltage spikes and reverse recovery losses of off-going output diodes. The capacitor voltage V_{Crr} and the resonant inductor current i_{Lr} can be found to be

$$V_{Crr} = \frac{1}{a}\left[V_S + \sqrt{(I_{RP}Z_{rr})^2 + V_S^2} \cdot \sin\left(\omega_{rr}t - \tan^{-1}\frac{V_S}{I_{RP}Z_{rr}}\right)\right] \tag{11}$$

$$i_{Lr} = I_O + \sqrt{I_{RP}^2 + (V_S/Z_{rr})^2} \cdot \cos\left(\omega_{rr}t - \tan^{-1}\frac{V_S}{I_{RP}Z_{rr}}\right) \quad (12)$$

$$\omega_{rr} = \sqrt{\frac{1}{L_rC_{rr}/a^2}} \quad (13)$$

$$Z_{rr} = \sqrt{L_ra^2/C_{rr}} \quad (14)$$

where $a = N_1/N_3$.

3) *Mode 3 (clamping):* The resonantly increasing capacitor voltage V_{Crr} is clamped to V_S and the excess stored energy in the resonant inductor L_r is delivered to the power supply V_S. Thus the resonant inductor current i_{Lr} decreases linearly toward I_O, or

$$L_r\frac{di_{Lr}}{dt} = V_S(1-a) - 2V_{\text{FET.on}} - 2aV_{D.\text{on}}. \quad (15)$$

4) *Mode 4 (powering):* In this mode, power is transferred from source to load similar to the powering stage of the conventional switched mode PWM converter:

$$I_O(t) = I_O(t_3) + \frac{V_S}{L_r + L_O}t \quad (16)$$

$$i_{Lr}(t) = I_O + \frac{V_SL_r/(L_o + L_r)}{Z_{rr}}\sin(\omega_{rr}t). \quad (17)$$

Since $V_S(1-a)/Z_{rr}$ is usually designed much smaller than I_O, the resonant inductor current i_{Lr} is limited to the output current I_O, which varies smoothly. The capacitor voltage V_{Crr} resonates with small amount of energy and finally decays to $V_S - (V_S - V_O)L_r/(L_r + L_O)$, which is determined by the divided voltage between the series-connected L_r and L_O. After a finite time-interval T_{on}, switch S_1 is turned off under the zero voltage-switching condition.

5) *Mode 5 (resonant):* By turning off switch S1, the current path is altered from switch S1 to capacitors C_1 and C_3. The series-connected resonant and filter inductors are partially resonant with the capacitors C_1, C_3, and C_{rr} and the capacitor voltage v_{C3} begins to decrease from the source voltage, that is,

$$V_{C3} = V_S - \frac{I_O}{2C_r + C_{rr}/a^2}\left(t + \frac{C_{rr}}{2C_ra^2\omega_p}\sin\omega_pt\right) + \frac{(V_S - V_O)L_r}{2C_r\omega_pZ_p(L_O + L_r)}(1 - \cos\omega_pt) \quad (18)$$

$$V_{Crr} = \frac{1}{a}\left[V_S - \frac{L_r(V_S - V_O)}{L_O + L_r} - \frac{I_O(t + 1/\omega_p\sin\omega_pt)}{2C_r + C_{rr}/a^2} + \frac{(V_S - V_O)L_r}{C_{rr}/a^2\omega_pZ_P(L_O + L_r)}(1 - \cos\omega_pt)\right] \quad (19)$$

$$\omega_p = \sqrt{\frac{2C_r + C_{rr}/a^2}{2C_rC_{rr}/a^2L_r}} \quad (20)$$

$$Z_p = \sqrt{\frac{L_r(2C_r + C_{rr}/a^2)}{2C_rC_{rr}/a^2}}. \quad (21)$$

When the capacitor voltage v_{C3} reaches zero, diode D3 begins to conduct and this mode ends (it is assumed that V_{C3} and V_{Crr} reach zero simultaneously despite the small difference. If the difference becomes large, one more should be added). In particular, the capacitor current i_{C3} flow only during this short interval and the voltampere reactive (VAR) ratings of the resonant capacitor are significantly reduced compared with those of the resonant type converter.

6) *Mode 6 (freewheeling):* This mode corresponds to the freewheeling mode of the conventional PWM dc/dc converter. During the above four modes, the resonant inductor and the output filter inductor are effectively series connected. Starting from this mode, two inductors are effectively decoupled through a short circuit of the output bridge diodes as shown in Fig. 2(c). The decoupling of the two inductors happens when L_r is chosen much smaller than L_O so that the rate of decrease of the current through L_r is much faster than that of L_O. The two inductor currents decrease linearly as

$$i_{Lr}(t) = i_{Lr}(t_5) - \frac{V_{D.\text{on}} + V_{\text{FET.on}}}{L_r}t \quad (22)$$

$$I_O(t) = I_O(t_5) - \frac{V_O}{L_O}t. \quad (23)$$

At proper time t_3, switch S4 is turned off under the zero voltage-switching condition and thus next mode starts.

7) *Mode 7 (resonant):* In this mode, resonant inductor L_r and switch capacitors C_2 and C_4 form an L-C resonant circuit, whereby the resonant inductor current i_{Lr} discharges and charges the capacitors C_2 and C_4. The resonant inductor current and capacitor voltage can be expressed as

$$i_{Lr}(t) = i_{Lr}(t_6)\cos\omega_rt \quad (24)$$

$$V_{C4}(t) = i_{Lr}(t_6)Z_r\sin\omega_rt \quad (25)$$

$$\omega_r = \sqrt{\frac{1}{L_r(2C_r)}} \quad (26)$$

$$Z_r = \sqrt{L_r/(2C_r)}. \quad (27)$$

To achieve a zero voltage-switching transient, inductor current i_{Lr} at the start of this mode must be large enough to charge up the capacitor C_4 fully from its initial value to the final V_S. This condition can be expressed by

$$L_ri_{Lr}(t_6)^2 > 2C_rV_S^2 \quad (28)$$

which is the necessary condition for ZVS of the primary switches [5].

8) *Mode 8 (linear decreasing):* When the capacitor voltage v_{C4} reaches V_S, diode D2 begin to conduct and the resonant inductor current i_{Lr} decreases linearly and rapidly as given by

$$i_{Lr}(t) = i_{Lr}(t_7) - \frac{V_s}{L_r}t. \tag{29}$$

The pretriggering signals of the switches S2 and S3 are initiated in order to ensure a zero voltage-switching condition at the start of the next cycle. When the resonant inductor current reaches zero, diodes D2 and D3 are turned off and switches S2 and S3 are turned on.

VI. Novel Features and Characteristics

The converter is designed for a maximum power $P_{o.\max}$ = 1.5 kW at 100 kHz of operating frequency. The proposed converter can be modeled as an equivalent circuit shown in Fig. 6 to obtain a dc conversion-ratio characteristic. The equivalent voltage V_{eq} of the dc output side obtained from referring the ac resonant input side is given as follows:6

$$V_{eq} = \begin{cases} aV_{Crr} \quad (V_{Crr}: (11)) & (t_1 < t < t_2) \quad (30) \\ aV_S & (t_2 < t < t_3) \quad (31) \\ V_S - \dfrac{L_r}{L_O + L_r}(V_S - V_O) & (t_3 < t < t_4) \quad (32) \\ aV_{Crr} \quad (V_{Crr}: (19)) & (t_4 < t < t_5). \quad (33) \end{cases}$$

The average output voltage V_O can be calculated as

$$V_O = \frac{1}{T}\int_{t_0}^{t_6} V_{eq}\, dt. \tag{34}$$

If the dc conversion ratio M and the duty ratio d are defined as

$$M = \frac{V_o}{V_s} \tag{35}$$

$$d = \frac{T_{on}}{T} \tag{36}$$

the dc conversion characteristics can be obtained. The dc characteristics are almost linear and load independent as shown in Fig. 6(c), better than those of any other similar converters. It deviates slightly from the characteristic curve (dotted line) of the PWM dc/dc converter depending on the load variations. The deviation arises from a little drop across the resonant inductor. The upper limit of the duty ratio can be extended to about 0.8–0.9 despite a linear-reversing current of the resonant inductor.

Fig. 7(a) shows normalized device voltage stress of the proposed converter comparing with those of several typical converters. The voltage stresses of the devices and components are always limited to the supply voltage V_S like a switched-mode PWM converter despite of the load variations.

Fig. 7(b) shows normalized device current stress of the proposed converter together with three other typical converters. The current stress is also clamped to the output current I_O. The current stress of the proposed converter is almost the same as that of the switched mode PWM converter and is much lower than those of any other converters such as the series-resonant converter, the resonant pole-type converter, and the ZCS quasi-resonant converter.

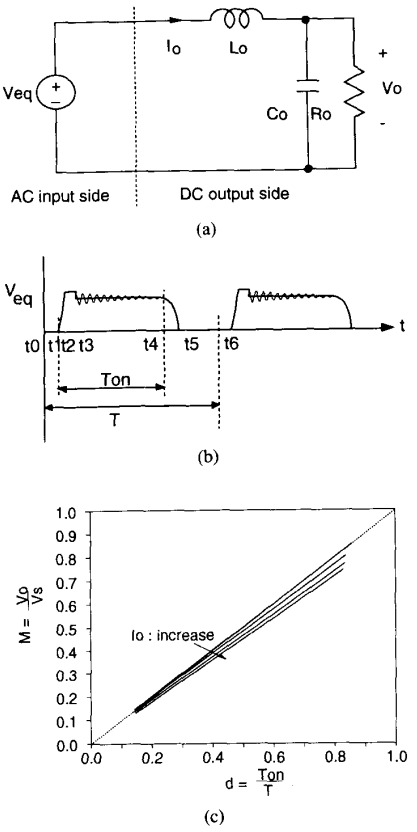

Fig. 6. DC conversion ratio derivation. (a) Equivalent circuit. (b) Equivalent waveform V_{eq} referred to the dc output side. (c) DC conversion ratio characteristics of the proposed converter for several values of I_O = 5, 10, 15, and 20 A.

It should also be stressed that the third auxiliary winding and the bridge diodes are connected to the supply side but not to the output capacitor side. By doing so, clamping operation is always guaranteed even if the supply voltage varies with large ripple because the clamp voltage will also follow the supply voltage variation. For comparison, if the clamp winding and the bridge diodes are connected to the output capacitor side, the clamping operation will not work properly when the supply voltage varies in a wide range because the output capacitor voltage and thus the clamp voltage will remain constant through the output voltage regulation. If the clamp voltage is fixed, a shoot-through phenomenon can occur through the auxiliary clamp winding and the bridge diodes to the output side when the supply voltage increases

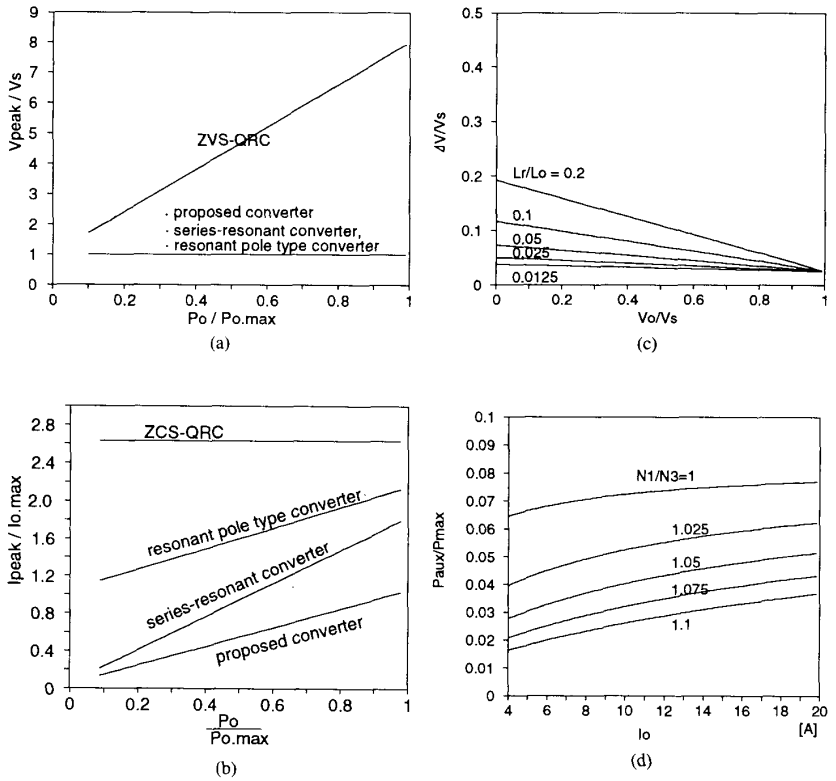

Fig. 7. Characteristics of proposed converter. (a) Comparisons of peak voltage stresses. (b) Peak current stresses with four different converters. (c) Normalized ripple voltage $\Delta V/V_S$ versus V_O/V_S for several L_r/L_O values at $N_1/N_3 = 1.025$. (d) Normalized handling power P_{aux} of the auxiliary circuit for several transformer turn ratios.

above a certain limit. In the proposed converter, the large voltage spikes of output diodes can simply and effectively be limited to $(N_1/N_3)V_S$ (almost $1 < N_1/N_3 < 1.1$). Fig. 4(b) shows the magnified waveform considering the reverse-recovery effect of the output diodes. These suppressed magnitude ΔV of the oscillatory ripple voltage can be found to be

$$\Delta V = V_S\left(a - \frac{L_O}{L_r + L_o}\right) - V_O\frac{L_r}{L_r + L_O}. \quad (37)$$

Fig. 7(c) shows the normalized ripple voltage $\Delta V/V_S$ for various L_r/L_o values. The normalized ripple voltage is very small and slightly dependent on V_O/V_S, and can be considered as

$$\Delta V = kV_S \qquad (k < 0.2). \quad (38)$$

Consequently, the large voltage spikes of the output diodes are adaptively and effectively limited by the auxiliary clamp circuit.

The auxiliary bridge diodes carry a triangular waveform current only during the clamping operation. Current waveforms i_{Da1} and i_{Da4} can be expressed as

$$i_{Da1}(i_{Da4}) = \frac{V_S(1-a) - 2V_{\text{FET.on}} - 2aV_{D.\text{on}}}{L_r}t + a\sqrt{I_{RP}^2 + (V_S/Z_{rr})^2}. \quad (39)$$

Then the average power rating of the auxiliary clamp circuit can be calculated as

$$P_{\text{aux.}} = \frac{V_s L_r\left[I_{RP}^2 + (V_S/Z_{rr})^2\right]}{2aT_s[V_S(1-a) - 2V_{\text{FET.on}} - 2aV_{D.\text{on}}]}. \quad (40)$$

Fig. 7(d) shows the average auxiliary power $P_{\text{aux.}}$ for various turn-ratio $a(= N_1/N_3)$ values, indicating that the power rating of auxiliary clamp circuit is influenced by the load current but low enough.

VII. Experimental Results

In this experiment, the proposed converter is designed for maximum output power $P_{o.\max} = 1.5$ kW at 100 kHz of operating frequency. The parameter values and the types of the devices used in the converter are as follows:

$$L_r = 15\ \mu H$$

$$C_r = 4.7\ nF$$

$$C_{rr} = 2.2\ nF$$

$$L_o = 100\ \mu H$$

MOSFET's $(S_1 - S_4)$: $IRF460$

Diodes $(D_{11} - D_{44})$: $BYT30PI1000$.

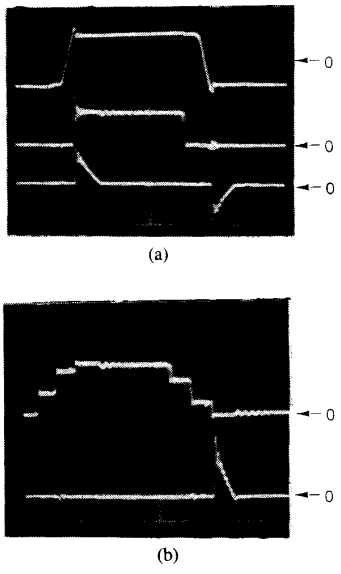

Fig. 8. Experimental waveforms. (a) Waveforms of resonant inductor current i_{Lr} (upper trace, 10 A/div, 2 μ sec/div), output diode voltage V_{D33} (middle trace, 50 V/div) and auxiliary diode current I_{Da1} (lower trace, 1 A/div) at V_s = 200 V, V_o = 50 V and I_o = 20 A. (b) Waveforms of auxiliary diode voltage (upper trace) and current (lower trace) at V_s = 200 V, V_o = 50 V and I_o = 20 A; 100 V/div, 1 A/div, 1 A/div, 2 μs/div.

The proposed converter is operated from the input power supply voltage of 200 V with the transformer turn ratios N_1:N_2 = 1:0.4 and N_1:N_3 = 1:1/1.025.

Fig. 8(a) shows the resonant inductor current i_{Lr}, output diode voltage V_{D33}, and auxiliary diode current I_{Da1}. As expected, the energy stored in the resonant inductor L_r during the reverse recovery process of the output diodes is seen to be effectively delivered to the supply voltage through the auxiliary bridge diodes. The voltage stress of the output diode is also seen to be clamped to a voltage level. Fig. 8(b) shows the waveform of the auxiliary bridge diodes verifying that the auxiliary diodes also switch at zero voltage conditions.

Fig. 9(b) shows the clamped waveforms of the output diode voltage emphasizing that the voltage stress of the proposed converter is lower than that of the preproposed converter. Small ringing still exists in Fig. 9(b), which is due to the transformer parasitics. Good clamping action of the circuit with C_{rr} requires a good coupling between the windings and a transformer with low leakage inductance. Fig. 9(c) and (d) shows the oscillograms of (c) output diode current and voltage and the extended waveform (d) of them only during turn-off transient. As anticipated, the turn-off loss is very low, resulting in high efficiency at high-frequency operation.

Fig. 10 shows the measured efficiency of the proposed converter in comparison with the preproposed one. The efficiency of the proposed converter with auxiliary circuit shows some improvement over the preproposed type. This

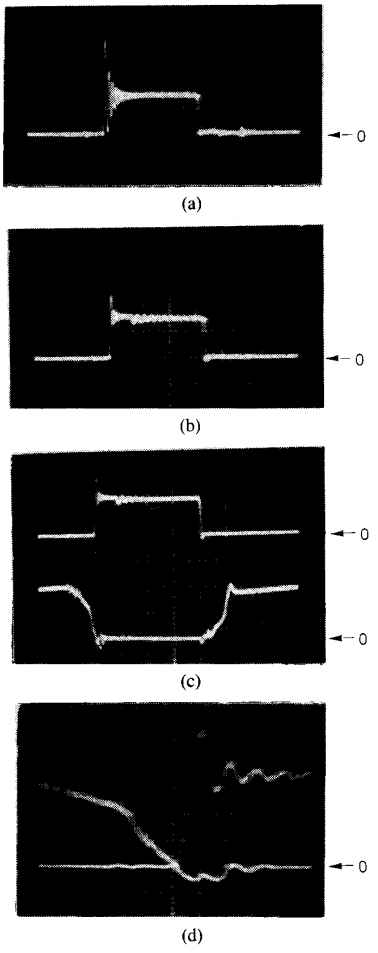

Fig. 9. Experimental waveforms. (a) Voltage waveforms of output diodes in preproposed converter. (b) Proposed converter; 50 V/div, 2 μ sec/div. (c) Output diode voltage (upper trace) and current (lower trace) of proposed converter, 50 V/div, 10 A/div. (d) Extended waveforms of picture (c) during the turn-off transient; 5 A/div, 20 V/div, 0.2 μ sec/div at V_s = 200 V, V_o = 50 V, and I_o = 20 A.

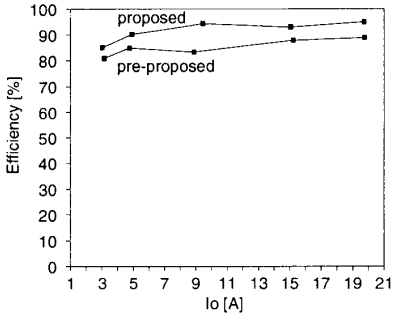

Fig. 10. Measured efficiency of proposed converter and preproposed converter as a function of load current.

improvement would be significant if the operating frequency is increased up to a megahertz range.

VIII. Conclusion

A new zero-voltage-switching constant frequency PWM dc/dc converter is proposed. The proposed converter has low VA ratings of the devices and components, constant switching frequency operation, and almost linear and load-independent dc conversion ratio characteristics. The voltage and current stresses are low and always limited to supply voltage V_S and output current I_O, respectively. Finally, the proposed converter has a low switching loss due to the zero voltage switchings for all of the devices including the output rectifier diodes, which makes the converter operable at high frequency with high efficiency. The features of the proposed converter are summarized as follows:

1) Almost linear and load-independent dc conversion ratio characteristic
2) Constant frequency PWM operation
3) Low voltage and low current stress
4) Low switching loss
5) Simple control
6) Low VAR ratings of the resonant elements
7) No reverse recovery problem of the diodes

References

[1] R. L. Steigerwald, "High-frequency resonant transistor dc-dc converters," *IEEE Trans. Ind. Electron.*, vol. IE-31, no. 2, pp. 181–191, May 1984.

[2] F. C. Schwarz, "An improved method of resonant current pulse modulation for power converters," *IEEE Trans. Ind. Electron. Con. Instr.*, vol. IECI-23, no. 2, pp. 133–141, May 1976.

[3] K. Liu, R. Oruganti, and F. C. Lee, "Quasi-resonant converters—Topologies and characteristics," *IEEE Trans. Power Electron.*, vol. PE-2, no. 1, pp. 62–71, Jan. 1987.

[4] R. W. De Doncker, D. M. Divan, and M. H. Kheraluwala, "A three-phase soft-switched high power density dc/dc converter for high power applications," *IEEE IAS Annu. Meeting Rec.*, 1988, pp. 796–804.

[5] C. P. Henze, H. C. Martin, and D. W. Parsley, "Zero voltage switching in high frequency power converters using pulse width modulation," in *Proc. IEEE Applied Power Electronics Conf. Rec.*, 1988, pp. 33–44.

[6] E. C. Nho and G. H. Cho, "A new zero-voltage zero-current mixed mode switching dc/dc converter with low device stresses," *IEEE IECON Conf. Rec.*, 1989, pp. 15–20.

In Dong Kim was born in Korea on Aug. 27, 1960. He received the B.S. degree in electrical engineering from Seoul National University, Seoul, Korea, in 1984. He received the M.S. and Ph.D. degrees in electrical engineering from the Korea Advanced Institute of Science and Technology (KAIST), Seoul, Korea, in 1987 and 1991, respectively.

Since 1991, he has been with the Rolling Stock R/D Center of Rolling Stock & Heavy Equipment Division of Daewoo Heavy Industries Ltd., Seoul, Korea. His research interests are induction motor drives, static power converters, and inverters and microprocessor-based system control.

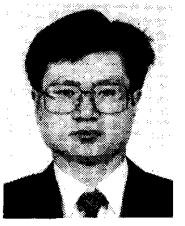

Eui Cheol Nho was born in Korea. He received the B.S. degree in electrical engineering from Seoul National University, Seoul, Korea, in 1984. He received the M.S. and Ph.D. degrees in electrical engineering from the Korea Advanced Institute of Science and Technology (KAIST), Seoul, Korea, in 1986 and 1991, respectively.

From 1986 to 1991, he worked for Cheongke Electromachinery Co. Since 1992, he has been with Power Tech Ltd. His research interests are induction motor drives, static power converters, and inverters and microprocessor-based system control.

Gyu Hyeong Cho (S'76–S'78–M'80) was born in Korea on April 19, 1953. He received the M.S. and Ph.D. degrees from the Korea Advanced Institute of Science and Technology (KAIST), Seoul, Korea, in 1977 and 1981, respectively.

During 1982–1983, he joined the Electronic Technology Division of Westinghouse R & D Center, Pittsburgh, PA, where he worked on unrestricted frequency changer systems and inverters. Since 1984, he has been an Assistant/Associate Professor in the Electrical Engineering Department of KAIST. His research interests are in the area of static power converters and drives, resonant converters, and integrated linear electronic circuit design.